

Contents lists available at SciVerse ScienceDirect

Physics Letters B

www.elsevier.com/locate/physletbNon-diagonal charged lepton mass matrix and non-zero θ_{13} J. Alberto Acosta^a, Alfredo Aranda^{a,b,*}, Manuel A. Buen-Abad^a, Alma D. Rojas^a^a Facultad de Ciencias, CUICBAS, Universidad de Colima, Colima, Mexico^b Dual C-P Institute of High Energy Physics, Mexico

ARTICLE INFO

Article history:

Received 8 September 2012

Received in revised form 10 December 2012

Accepted 17 December 2012

Available online 20 December 2012

Editor: T. Yanagida

ABSTRACT

Assuming that the neutrino mass matrix is diagonalized by the tribimaximal mixing matrix, we explore the textures for the charged lepton mass matrix that render a U_{PMNS} lepton mixing matrix consistent with data. In particular we are interested in finding the textures with the maximum number of zeros. We explore the cases of real matrices with three and four zeros and find that only ten matrices with three zeros provide solutions in agreement with data. We present the successful Yukawa textures including the relative sizes of their non-zero entries as well as some new and interesting relations among the entries of these textures in terms of the charged lepton masses. We also show that these relations can be obtained directly from a parametrization of the charged lepton mixing matrix U_l .

© 2012 Elsevier B.V. Open access under [CC BY license](http://creativecommons.org/licenses/by/4.0/).

1. Introduction

In the framework of discrete flavor symmetries one of the most used ansatz for the lepton mixing matrix U_{PMNS} is the tribimaximal mixing (TBM) matrix [1], which despite the non-zero value for θ_{13} recently confirmed by the T2K Collaboration [2], Double Chooz [3], Daya Bay [4] and RENO [5] experiments, can still be used as a good approximation. Contributions from the charged lepton sector and/or from renormalization effects, can generate a non-zero value for θ_{13} in agreement with the experimental data. For a classification of models predicting TBM mixing see [6,7] and the references therein, and for an overview of flavor symmetry models for neutrino mixing, based on non-Abelian discrete symmetries that give the TBM pattern, see Ref. [8].

Other ansatz for the neutrino mass matrix have been explored. One such case consists on the so-called n -zero textures where, for example, taking the case of Majorana neutrinos, it has been found that only two independent zero entries are allowed by current data [9,10]. For Dirac mass matrices the situation is different (since the mass matrices are not symmetric) as shown in [11], where a study of the minimal mass matrices with as many zeros as possible determined that up to five zero entries are allowed. In both of these cases the neutrino mass matrices were expressed in the charged lepton diagonal basis. Fritzsche-like [12] textures have also been considered for both the charged lepton and neutrino mass matrices in [13], where Dirac neutrinos are considered, and in [14], where all possible Hermitian six-zero¹ Fritzsche-like as well as non-Fritzsche-like textures for lepton mass matrices have been investigated, for both Majorana and Dirac matrices. For a recent overview of all possible cases of Fritzsche-like as well as non-Fritzsche-like matrices as possible textures of the fermion mass matrices see [15].

In this Letter we take the following approach: assuming that the neutrino mass matrix is diagonalized by the TBM matrix, we determine the textures for the charged lepton mass matrix that leads to a lepton mixing matrix in agreement with the experimental data. We find both the number and location of zeros in the charged lepton mass matrix as well as the relative sizes of the non-zero entries in the corresponding Yukawa matrix. The results obtained can be of use to model builders interested in obtaining flavor models with TBM mixing in the neutrino sector.

In Section 2 we present the general idea and setup of our analysis. The n -zero textures for $n = 3$ are obtained in Section 3. Section 4 contains a description of the numerical analysis performed, as well as our results and discussion. Finally, Section 5 contains our conclusions.

* Corresponding author at: Facultad de Ciencias, CUICBAS, Universidad de Colima, Colima, Mexico.

E-mail addresses: kripton0x@gmail.com (J.A. Acosta), fefo@uocol.mx (A. Aranda), manuelbuenabadnajar@gmail.com (M.A. Buen-Abad), alma.drp@gmail.com (A.D. Rojas).¹ Here the counting of zeros refers to the total number of independent zeros in both the charged lepton and neutrino mass matrices.

2. The setup

The lepton mixing matrix U_{PMNS} is given by

$$U_{PMNS} = U_l^\dagger U_\nu, \quad (1)$$

where U_l relates left-handed leptons in the weak basis e_l to the mass basis leptons e'_l : $e'_l = U_l e_l$; and U_ν corresponds to the same basis transformation for left-handed neutrinos $\nu'_l = U_\nu \nu_l$.

The U_{PMNS} matrix can be parametrized as follows [16]:

$$U_{PMNS} = \begin{pmatrix} c_{12}c_{13} & s_{12}c_{13} & s_{13}e^{-i\delta} \\ -s_{12}c_{23} - c_{12}s_{23}s_{13}e^{i\delta} & c_{12}c_{23} - s_{12}s_{23}s_{13}e^{i\delta} & s_{23}c_{13} \\ s_{12}s_{23} - c_{12}c_{23}s_{13}e^{i\delta} & -c_{12}s_{23} - s_{12}c_{23}s_{13}e^{i\delta} & c_{23}c_{13} \end{pmatrix} \quad (2)$$

where $s_{ij} = \sin \theta_{ij}$, $c_{ij} = \cos \theta_{ij}$ and δ is the Dirac CP-violating phase.

Since the U matrices in (1) are unitary, we can express U_l as

$$U_l = U_\nu U_{PMNS}^\dagger. \quad (3)$$

In our approach, we demand that U_ν be the TBM matrix, namely

$$U_\nu = U_{TBM} = \begin{pmatrix} \sqrt{\frac{2}{3}} & \frac{1}{\sqrt{3}} & 0 \\ -\frac{1}{\sqrt{6}} & \frac{1}{\sqrt{3}} & -\frac{1}{\sqrt{2}} \\ -\frac{1}{\sqrt{6}} & \frac{1}{\sqrt{3}} & \frac{1}{\sqrt{2}} \end{pmatrix}, \quad (4)$$

and so, if $U_\nu = U_{TBM}$ is the matrix that diagonalizes the neutrino mass matrix M_ν and U_l the one that diagonalizes the squared charged lepton mass matrix $M_l^2 \equiv M_l M_l^\dagger$, we want to determine the form of M_l such that $U_{PMNS} = U_l^\dagger U_{TBM}$ has values in the allowed experimental range.

As described above the matrix U_l diagonalizes M_l^2 and thus satisfies

$$M_l^2 = U_l M_{ID}^2 U_l^\dagger \quad (5)$$

where $M_{ID} = \text{diag}(m_e, m_\mu, m_\tau)$ and $M_{ID}^2 \equiv M_{ID} M_{ID}^\dagger$.

At this point M_l is an arbitrary mass matrix with unknown values and we parametrize it as

$$M_l = \begin{pmatrix} a & b & c \\ d & e & f \\ g & h & i \end{pmatrix}. \quad (6)$$

In general the mass matrix M_l has complex entries, however, in this first approach we consider the particular case of a real mass matrix and thus assume all parameters in M_l to be real. In this particular case, Eq. (5) becomes a set of equations for the entries of M_l^2 :

$$\begin{pmatrix} a^2 + b^2 + c^2 & ad + be + cf & ag + bh + ci \\ ad + be + cf & d^2 + e^2 + f^2 & dg + eh + fi \\ ag + bh + ci & dg + eh + fi & g^2 + h^2 + i^2 \end{pmatrix}. \quad (7)$$

There are nine variables and only six equations encoded in Eq. (5). Thus we have an incomplete set of equations. To proceed we can start by making some assumptions on the form of the lepton mass matrix. Just as an example take M_l to be a lower triangular matrix (by making $b = c = f = 0$). This gives

$$M_l M_l^\dagger = \begin{pmatrix} a^2 & ad & ag \\ ad & d^2 + e^2 & dg + eh \\ ag & dg + eh & g^2 + h^2 + i^2 \end{pmatrix}. \quad (8)$$

The number of variables has now been reduced to six variables, and with the six independent equations (as we show later in the Letter) it is easy to find solutions for the parameters in Eq. (8) in agreement with the experimental data.

We are interested in determining the textures with the maximum number of zeros. The main motivation for this is that having such textures can be useful to model builders interested in obtaining them using an underlying flavor symmetry. With this in mind, we explore the textures with the maximum number of zeros such that Eq. (5) has real solutions in the allowed experimental range for the mixing angles. Note that our assumption of real mass matrices implies that in our case the CP-violating phase satisfies $\delta = 0$ or π . We also assume that the Majorana CP-violating phases are zero but note however, that since they can be factorized from U_{PMNS} as a diagonal matrix, their inclusion would not affect the magnitudes of the U_{PMNS} entries.

3. Finding the textures

We are concerned with the possible textures for the non-diagonal mass matrix for charged leptons (as we said before, assuming that the neutrino mass matrix is diagonalized by the TBM matrix). We assume that the entries are real and so $M_l M_l^\dagger = M_l M_l^T$. Zeros in the entries of our matrices may be due to some underlying symmetry(ies) and because of that we will look for the textures with the highest possible number of zeros.

As discussed above, we have a system of six coupled, quadratic equations and (in general) nine variables. Thus there is a need for some extra constraints on the variables. For matrices with no zeros at all we need three of this extra constraints, for matrices with one zero we need only two. We begin our analysis with three-zero mass matrices requiring no extra constraints.

A combinatorial analysis shows that, for the three-zero matrices, we have $\binom{9}{3} = 84$ ways to place the three zeros and thus 84 different matrix forms. Nevertheless, it is well known that in forming the real product $M_l M_l^T$, any permutation of the columns of the matrix involved does not change the resulting product matrix. Thus, this reduces the number of matrices to 20. From these textures we discard those with a row or column made of zeros because they are singular. There are 4 cases of this and we are left with only 16 different textures. Another condition that has to be satisfied, in view of the non-zero values for the charged lepton masses, is $\text{Tr}(M_l M_l^T) \neq 0$.

Denoting the possible mass matrices by M_{nk} , where indexes stand for the k th texture of the non-diagonalized charged lepton matrix with n -zeros, for $n = 3$ we obtain:

$$\begin{aligned}
 M_{301} &= \begin{pmatrix} 0 & 0 & c \\ d & e & 0 \\ g & h & i \end{pmatrix}; & M_{302} &= \begin{pmatrix} 0 & 0 & c \\ d & e & f \\ g & h & 0 \end{pmatrix}; & M_{303} &= \begin{pmatrix} 0 & b & c \\ d & 0 & 0 \\ g & h & i \end{pmatrix}; & M_{304} &= \begin{pmatrix} 0 & b & c \\ d & 0 & f \\ g & h & 0 \end{pmatrix}; \\
 M_{305} &= \begin{pmatrix} 0 & b & c \\ d & e & f \\ g & 0 & 0 \end{pmatrix}; & M_{306} &= \begin{pmatrix} a & b & c \\ 0 & 0 & f \\ g & h & 0 \end{pmatrix}; & M_{307} &= \begin{pmatrix} a & b & c \\ 0 & e & f \\ g & 0 & 0 \end{pmatrix}; & M_{308} &= \begin{pmatrix} 0 & b & c \\ 0 & e & f \\ g & 0 & i \end{pmatrix}; \\
 M_{309} &= \begin{pmatrix} 0 & b & c \\ 0 & 0 & f \\ g & h & i \end{pmatrix}; & M_{310} &= \begin{pmatrix} a & 0 & 0 \\ d & e & 0 \\ g & h & i \end{pmatrix}; & M_{311} &= \begin{pmatrix} 0 & b & c \\ d & e & f \\ 0 & 0 & i \end{pmatrix}; & M_{312} &= \begin{pmatrix} 0 & b & c \\ d & 0 & f \\ 0 & h & i \end{pmatrix}; \\
 M_{313} &= \begin{pmatrix} 0 & 0 & c \\ d & e & f \\ 0 & h & i \end{pmatrix}; & M_{314} &= \begin{pmatrix} a & b & c \\ 0 & e & f \\ 0 & 0 & i \end{pmatrix}; & M_{315} &= \begin{pmatrix} a & b & c \\ 0 & 0 & f \\ 0 & h & i \end{pmatrix}; & M_{316} &= \begin{pmatrix} a & 0 & c \\ 0 & e & f \\ 0 & h & i \end{pmatrix}.
 \end{aligned} \tag{9}$$

As none of the matrices shown above is obtained from another by means of permuting columns, these are all the possible three-zero textures to be analyzed.

4. Analysis

We are interested in identifying the textures which provide solutions to Eq. (5). In order to find which textures provide solutions we performed (for each texture) a scan over the whole allowed experimental range for the mixing angles taking the values $\delta = 0$ and $\delta = \pi$ for the CP-violating phase.

To carry out the numerical analysis we used the experimental data at 3σ from the global neutrino data analysis [17]

	Best fit value	3σ range
$\sin^2 \theta_{12}$	0.312	0.27–0.36
$\sin^2 \theta_{23}$	0.52	0.39–0.64
δ	-0.61π	$0-2\pi$
	(-0.41π)	

with normal (inverted) hierarchy, and the recently Daya Bay results [5] (confirmed at 5σ)

$$\sin^2 2\theta_{13} = 0.092 \pm 0.017, \tag{11}$$

which can be rewritten as $\sin^2 \theta_{13} = 0.0235 \pm 0.0045$.

For the charged leptons masses we use the values given in [16]

$$m_e = 0.510998910 \pm 0.000000013 \text{ MeV}, \quad m_\mu = 105.658367 \pm 0.000004 \text{ MeV}, \quad m_\tau = 1776.82 \pm 0.16 \text{ MeV}. \tag{12}$$

For instance by taking the central values of the mixing angles and those of the charged lepton masses (setting $\delta = 0$) we obtain

$$U_{PMNS} = \begin{pmatrix} 0.819631 & 0.551952 & 0.153476 \\ -0.478787 & 0.512846 & 0.712567 \\ 0.314593 & -0.657524 & 0.684612 \end{pmatrix}, \tag{13}$$

and from Eq. (3) we get for U_l

$$U_l = \begin{pmatrix} 0.987895 & -0.0948358 & -0.122758 \\ -0.124467 & -0.0123053 & -0.992147 \\ 0.0925805 & 0.995417 & -0.0239603 \end{pmatrix}. \tag{14}$$

If we use these values for the example of the lower triangular matrix presented in Section 2, equating Eq. (8) to the explicit value of the right-hand side of Eq. (5), and using Eq. (14) and M_{ID}^2 evaluated at the central value for the lepton masses, we find:

$$|M_l| = \begin{pmatrix} 218.35 & 0 & 0 \\ 1761.06 & 79.71 & 0 \\ 37.70 & 106.87 & 5.51 \end{pmatrix}, \quad |Y_l| = \begin{pmatrix} 8.8 \times 10^{-4} & 0 & 0 \\ 7.2 \times 10^{-3} & 3.2 \times 10^{-4} & 0 \\ 1.5 \times 10^{-4} & 4.3 \times 10^{-4} & 2.0 \times 10^{-5} \end{pmatrix}; \quad (15)$$

where $|M_l|$ is in MeV and the Yukawa matrix Y_l shown above is obtained from:

$$Y_l = \frac{1}{\langle H \rangle} M_l, \quad (16)$$

being $\langle H \rangle \approx 246$ GeV the vacuum expectation value (VEV) of the Higgs field [16] (here we are assuming only one Higgs doublet contributes to the mass matrix. In general in this Letter we assume either that, or if there are more SU(2) doublets involved, that they all acquire VEV's of $O(10^2)$ GeV).

To perform the complete scan we used a grid of dimensions $30 \times 30 \times 30$ in the experimental range of the three mixing angles. For each combination of the mixing angles that provides solutions to Eq. (5), we select only the real solutions. Once those are determined, we then also determine the order of magnitude of the Yukawa mass entries by finding their minimum and maximum values.

4.1. Results for three-zero textures

From all the possible three-zero textures (shown in Eq. (9)) only the following provide (real) solutions: $M_{304}, M_{308}, M_{309}, M_{310}, M_{311}, M_{312}, M_{313}, M_{314}, M_{315}$, and M_{316} .

For the textures $M_{301}, M_{302}, M_{303}, M_{305}, M_{306}$, and M_{307} we did not find any solution. The reason is that all these textures lead to an extra constriction because the matrix product $M_l M_l^T$ has a zero entry. Those entries are $(M_{301} M_{301}^T)_{12}, (M_{302} M_{302}^T)_{13}, (M_{303} M_{303}^T)_{12}, (M_{305} M_{305}^T)_{13}, (M_{306} M_{306}^T)_{23}$, and $(M_{307} M_{307}^T)_{23}$.

As mentioned above, once we have performed all calculations (including the normalization of the mass matrix by the VEV of the Higgs field) we find the maximum and minimum orders of magnitude of the entries for each texture of the Yukawa matrix. They are shown here (up to $O(1)$ coefficients):

Y	$\delta = 0$	$\delta = \pi$
$ Y_{304} \sim$	$\begin{pmatrix} 0 & 10^{-7}-10^{-5} & 10^{-3} \\ 10^{-6}-10^{-3} & 0 & 10^{-2} \\ 10^{-6}-10^{-4} & 10^{-7}-10^{-4} & 0 \end{pmatrix};$	$\begin{pmatrix} 0 & 10^{-6}-10^{-4} & 10^{-4}-10^{-3} \\ 10^{-5}-10^{-3} & 0 & 10^{-2} \\ 10^{-5}-10^{-4} & 10^{-6}-10^{-3} & 0 \end{pmatrix};$
$ Y_{308} \sim$	$\begin{pmatrix} 0 & 10^{-4}-10^{-3} & 10^{-9}-10^{-3} \\ 0 & 10^{-3}-10^{-2} & 10^{-7}-10^{-2} \\ 10^{-5} & 0 & 10^{-4}-10^{-3} \end{pmatrix};$	$\begin{pmatrix} 0 & 10^{-4}-10^{-3} & 10^{-9}-10^{-3} \\ 0 & 10^{-3}-10^{-2} & 10^{-7}-10^{-2} \\ 10^{-5} & 0 & 10^{-4}-10^{-3} \end{pmatrix};$
$ Y_{309} \sim$	$\begin{pmatrix} 0 & 10^{-5}-10^{-4} & 10^{-4}-10^{-3} \\ 0 & 0 & 10^{-2} \\ 10^{-5} & 10^{-4} & 10^{-9}-10^{-3} \end{pmatrix};$	$\begin{pmatrix} 0 & 10^{-5}-10^{-4} & 10^{-4}-10^{-3} \\ 0 & 0 & 10^{-2} \\ 10^{-5} & 10^{-4} & 10^{-8}-10^{-3} \end{pmatrix};$
$ Y_{310} \sim$	$\begin{pmatrix} 10^{-4}-10^{-3} & 0 & 0 \\ 10^{-2} & 10^{-4}-10^{-3} & 0 \\ 10^{-9}-10^{-3} & 10^{-4}-10^{-3} & 10^{-5} \end{pmatrix};$	$\begin{pmatrix} 10^{-4}-10^{-3} & 0 & 0 \\ 10^{-2} & 10^{-4}-10^{-3} & 0 \\ 10^{-9}-10^{-3} & 10^{-4}-10^{-3} & 10^{-5} \end{pmatrix};$
$ Y_{311} \sim$	$\begin{pmatrix} 0 & 10^{-4}-10^{-3} & 10^{-9}-10^{-3} \\ 10^{-5} & 10^{-3}-10^{-2} & 10^{-7}-10^{-2} \\ 0 & 0 & 10^{-4}-10^{-3} \end{pmatrix};$	$\begin{pmatrix} 0 & 10^{-4}-10^{-3} & 10^{-9}-10^{-3} \\ 10^{-5} & 10^{-3}-10^{-2} & 10^{-7}-10^{-2} \\ 0 & 0 & 10^{-4}-10^{-3} \end{pmatrix};$
$ Y_{312} \sim$	$\begin{pmatrix} 0 & 10^{-5}-10^{-4} & 10^{-4}-10^{-3} \\ 10^{-5} & 0 & 10^{-2} \\ 0 & 10^{-4} & 10^{-9}-10^{-3} \end{pmatrix};$	$\begin{pmatrix} 0 & 10^{-5}-10^{-4} & 10^{-4}-10^{-3} \\ 10^{-5} & 0 & 10^{-2} \\ 0 & 10^{-4} & 10^{-8}-10^{-3} \end{pmatrix};$
$ Y_{313} \sim$	$\begin{pmatrix} 0 & 0 & 10^{-4}-10^{-3} \\ 10^{-5} & 10^{-4}-10^{-3} & 10^{-2} \\ 0 & 10^{-4}-10^{-3} & 10^{-9}-10^{-3} \end{pmatrix};$	$\begin{pmatrix} 0 & 0 & 10^{-4}-10^{-3} \\ 10^{-5} & 10^{-4}-10^{-3} & 10^{-2} \\ 0 & 10^{-4}-10^{-3} & 10^{-9}-10^{-3} \end{pmatrix};$
$ Y_{314} \sim$	$\begin{pmatrix} 10^{-6} & 10^{-4}-10^{-3} & 10^{-9}-10^{-3} \\ 0 & 10^{-3}-10^{-2} & 10^{-7}-10^{-2} \\ 0 & 0 & 10^{-4}-10^{-3} \end{pmatrix};$	$\begin{pmatrix} 10^{-6} & 10^{-4}-10^{-3} & 10^{-9}-10^{-3} \\ 0 & 10^{-3}-10^{-2} & 10^{-7}-10^{-2} \\ 0 & 0 & 10^{-4}-10^{-3} \end{pmatrix};$
$ Y_{315} \sim$	$\begin{pmatrix} 10^{-6} & 10^{-5}-10^{-4} & 10^{-4}-10^{-3} \\ 0 & 0 & 10^{-2} \\ 0 & 10^{-4} & 10^{-9}-10^{-3} \end{pmatrix};$	$\begin{pmatrix} 10^{-6} & 10^{-5}-10^{-4} & 10^{-4}-10^{-3} \\ 0 & 0 & 10^{-2} \\ 0 & 10^{-4} & 10^{-8}-10^{-3} \end{pmatrix};$
$ Y_{316} \sim$	$\begin{pmatrix} 10^{-6} & 0 & 10^{-4}-10^{-3} \\ 0 & 10^{-4}-10^{-3} & 10^{-2} \\ 0 & 10^{-4}-10^{-3} & 10^{-9}-10^{-3} \end{pmatrix};$	$\begin{pmatrix} 10^{-6} & 0 & 10^{-4}-10^{-3} \\ 0 & 10^{-4}-10^{-3} & 10^{-2} \\ 0 & 10^{-4}-10^{-3} & 10^{-9}-10^{-3} \end{pmatrix}.$

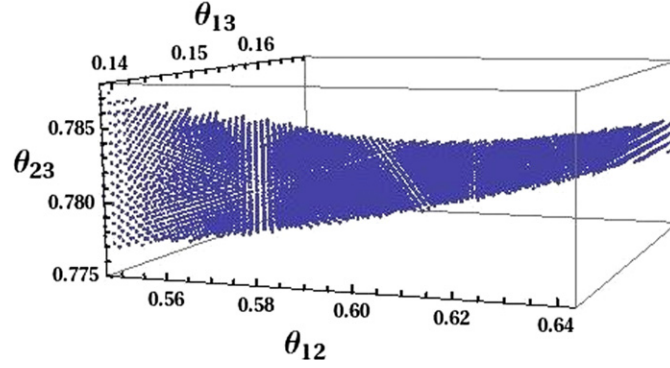


Fig. 1. Solution volume of M_{304} for $\delta = \pi$, found with a grid of $40 \times 40 \times 40$. Similar results are obtained for $\delta = 0$.

4.2. Solution volume

As part of the analysis we performed, we searched for the solution volume of each three-zero texture, that is, the set of points given by the three mixing angles that make possible to find real solutions to the entries of the M_l matrix.

In the case of textures $M_{308} - M_{316}$ the solution volume fills the complete space given by the experimental intervals of the three mixing angles (the experimentally allowed parameter space). This happens for both $\delta = 0$ and $\delta = \pi$.

The most interesting case is the texture M_{304} , which has the zeros on the major diagonal (and its permutations). The relevance of this case is that the angle θ_{23} is now very restricted. Thus, we took a closer look within a smaller interval for θ_{23} using a finer grid of $40 \times 40 \times 40$, and analyzing a θ_{23} interval of $[0.7745, 0.7950]$, we find that the solution volume of M_{304} , for both $\delta = 0$ and $\delta = \pi$, is a thin curved surface (presented in Fig. 1 for $\delta = \pi$); the only difference between these two cases is a displacement of the interval allowed for θ_{23} , which is $[0.7763, 0.7876]$ for $\delta = 0$, and $[0.7750, 0.7873]$ for $\delta = \pi$. These intervals are near but exclude the central value of θ_{23} .

4.3. A parametrization for U_l

The Yukawa matrices in (16) can explicitly be written as

$$Y_l = \begin{pmatrix} y_a & y_b & y_c \\ y_d & y_e & y_f \\ y_g & y_h & y_i \end{pmatrix}. \tag{17}$$

Then, the diagonal entries $(Y_l Y_l^T)_{ii}$ are just the sum of the square of the elements of the i th row of Y_l :

$$(Y_l Y_l^T)_{11} = y_a^2 + y_b^2 + y_c^2, \quad (Y_l Y_l^T)_{22} = y_d^2 + y_e^2 + y_f^2, \quad (Y_l Y_l^T)_{33} = y_g^2 + y_h^2 + y_i^2. \tag{18}$$

The textures obtained in Subsection 4.1 present some interesting features: first note that in all textures the largest upper bound (10^{-2}) always appears in the second row. Thus, from Eq. (18), $(Y_l Y_l^T)_{22} \sim O(10^{-4})$. This is a little higher than $O(m_\mu^2 / \langle H \rangle^2 \sim 5 \times 10^{-5})$. Note also that (except for the Y_{304}) the third row has always an upper bound of 10^{-3} and then, from Eq. (18), we can deduce that $(Y_l Y_l^T)_{33} \sim O(10^{-6})$. This is quite close to the value of the ratio $m_\mu^2 / \langle H \rangle^2 \sim 10^{-7}$. More precisely and using the explicit values of the Yukawa matrix of Eq. (15) we find

$$y_a^2 + y_b^2 + y_c^2 = 7.7 \times 10^{-7}, \quad y_d^2 + y_e^2 + y_f^2 = 5.2 \times 10^{-5}, \quad y_g^2 + y_h^2 + y_i^2 = 2.1 \times 10^{-7}. \tag{19}$$

We thus find that there are extra conditions on the entries of Y_l in terms of the charged leptons masses. Because of Eq. (5), we can expect that these conditions may be due to an internal structure of the mixing matrix U_l for the charged leptons. In what follows we show that there is indeed a parametrization for this matrix that leads to specific relations between the entries in the Yukawa matrices and the charged lepton masses that reproduce the above results, including the small deviations in the orders of magnitude.

Motivated by the fact that the charged leptons are analogous to the down type quarks in terms of representations of the Standard Model gauge group, we consider a CKM-like parametrization for the U_l mixing matrix in terms of the three angles θ_{12}^l , θ_{13}^l and θ_{23}^l , taking values between 0 and $\pi/2$, and all phases set to zero in order to use real values for the U_l matrix, as we have done in the whole analysis. Then, we can write:

$$U_l = \begin{pmatrix} 1 & 0 & 0 \\ 0 & \cos \theta_{23}^l & \sin \theta_{23}^l \\ 0 & -\sin \theta_{23}^l & \cos \theta_{23}^l \end{pmatrix} \begin{pmatrix} \cos \theta_{13}^l & 0 & \sin \theta_{13}^l \\ 0 & 1 & 0 \\ -\sin \theta_{13}^l & 0 & \cos \theta_{13}^l \end{pmatrix} \begin{pmatrix} \cos \theta_{12}^l & \sin \theta_{12}^l & 0 \\ -\sin \theta_{12}^l & \cos \theta_{12}^l & 0 \\ 0 & 0 & 1 \end{pmatrix}. \tag{20}$$

Using U' instead of U_{PMNS} (to avoid agglomeration of indexes) one can easily find that:

$$\sin^2 \theta_{13} = 1 - (U'_{11})^2 - (U'_{12})^2, \tag{21}$$

$$\sin^2 \theta_{23} = \frac{(U'_{23})^2}{(U'_{11})^2 + (U'_{12})^2}, \tag{22}$$

$$\sin^2 \theta_{12} = \frac{(U'_{12})^2}{(U'_{11})^2 + (U'_{12})^2}. \tag{23}$$

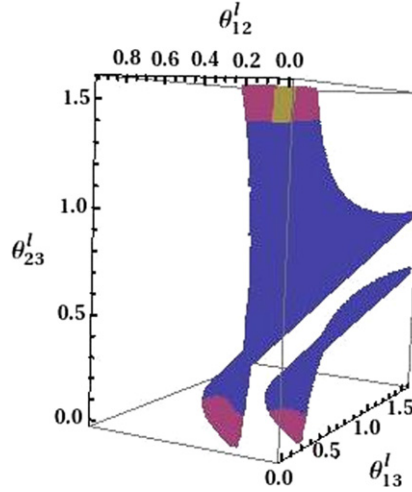


Fig. 2. Sets of values for the angles of the charged lepton mixing matrix that match the experimental results (see description in text). The yellow (light) band in the upper part of the plot is the region consistent with all experimental results. (For interpretation of the references to color, the reader is referred to the web version of this Letter.)

Here the θ_{ij} are, as before, the parameters of U_{PMNS} ; different from θ_{ij}^l , which parametrize U_l . We evaluated Eqs. (21)–(23) with $\theta_{ij}^l \in [0, \pi/2]$, and took all the points that matched the experimental intervals given by (10) and (11). The points $(\theta_{23}^l, \theta_{13}^l, \theta_{12}^l)$ are presented in Fig. 2.

In Fig. 2 the blue region is made of those values of the angles that solve Eq. (21) within the experimental values, the purple points are those that solve Eqs. (21) and (22) within the experimental ranges, and the dark yellow region is the set of points that satisfies the three equations (21), (22) and (23) within all the experimental values. We then obtain a small region given by two small angles and a large one:

$$\theta_{12}^l = [0.06-0.15], \quad \theta_{13}^l = [0.07-0.16], \quad \theta_{23}^l = [1.43-1.57 \approx (\pi/2)]. \quad (24)$$

Now we use the parametrization of the U_l matrix given by Eq. (20) and the values of its angles to make an analysis of the entries in a general charged lepton mass matrix, of the form given by (6). Let us remember that U_l appears in (5). Using the values given in (24), one can build a simpler form for U_l . Indeed, according to Eq. (20) and using the fact that θ_{12}^l and θ_{13}^l are small, we can use a first-order approximation for their respective rotation matrices. The size of the angle θ_{23}^l allows us to use a first-order approximation too, but around $\theta_{23}^l = \pi/2$. Then, $\sin(\theta_{23}^l) \approx 1$ and $\cos(\theta_{23}^l) \approx \frac{\pi}{2} - \theta_{23}^l \equiv \epsilon$. Thus, we end up with:

$$U_l \approx \begin{pmatrix} 1 & 0 & 0 \\ 0 & \epsilon & 1 \\ 0 & -1 & \epsilon \end{pmatrix} \begin{pmatrix} 1 & 0 & \theta_{13}^l \\ 0 & 1 & 0 \\ -\theta_{13}^l & 0 & 1 \end{pmatrix} \begin{pmatrix} 1 & \theta_{12}^l & 0 \\ -\theta_{12}^l & 1 & 0 \\ 0 & 0 & 1 \end{pmatrix}. \quad (25)$$

Using (25) in (5), we obtain the matrix M_l^2 in terms of θ_{12}^l , θ_{13}^l and ϵ . Comparing the result with (7), we can see that the variables from the first row of the mass matrix must satisfy:

$$a^2 + b^2 + c^2 \approx m_e^2 + m_\mu^2 \theta_{12}^{l2} + m_\tau^2 \theta_{13}^{l2} \quad (26)$$

the variables of the second row of (6) satisfy:

$$d^2 + e^2 + f^2 \approx m_\tau^2 + m_e^2 (-\epsilon \theta_{12}^l - \theta_{13}^l)^2 + m_\mu^2 (\epsilon - \theta_{12}^l \theta_{13}^l)^2 \sim m_\tau^2 \quad (27)$$

and the third row of (6) must have a contribution of the form

$$g^2 + h^2 + i^2 \approx m_\tau^2 \epsilon^2 + m_e^2 (\theta_{12}^l - \epsilon \theta_{13}^l)^2 + m_\mu^2 (-1 - \epsilon \theta_{12}^l \theta_{13}^l)^2 \sim m_\mu^2. \quad (28)$$

These expressions explain the observations considered at the beginning of the present subsection, including the corrections to the order of magnitude estimates, and represent the main result of this analysis.

Taking our specific example above, dividing Eqs. (26)–(28) by $\langle H \rangle^2$ as in (16), and using the values $\theta_{12}^l = 0.09$, $\theta_{13}^l = 0.1215$, $\theta_{23}^l = 1.55$ as well as the central values for the charged lepton masses we have:

$$\begin{aligned} \frac{1}{\langle H \rangle^2} (m_e^2 + m_\mu^2 \theta_{12}^{l2} + m_\tau^2 \theta_{13}^{l2}) &= 7.7 \times 10^{-7}, \\ \frac{1}{\langle H \rangle^2} (m_\tau^2 + m_e^2 (-\epsilon \theta_{12}^l - \theta_{13}^l)^2 + m_\mu^2 (\epsilon - \theta_{12}^l \theta_{13}^l)^2) &= 5.2 \times 10^{-5}, \\ \frac{1}{\langle H \rangle^2} (m_\tau^2 \epsilon^2 + m_e^2 (\theta_{12}^l - \epsilon \theta_{13}^l)^2 + m_\mu^2 (-1 - \epsilon \theta_{12}^l \theta_{13}^l)^2) &= 2.1 \times 10^{-7}. \end{aligned} \quad (29)$$

These are the values from (19), which are relations that exhibit the dependence of the entries of Y_l on the masses and the mixing angles of U_l . It is easily observed that for the first row, although the leading term (zeroth order on the angles) is m_e^2 , the other contributions play a more important role than this one, because the masses of the μ and τ leptons are much greater than that of the electron and even overcome the small size of their coefficients (which are powers of the angles). Finally, we note that these expressions are independent of the texture chosen for the Yukawa matrix and also independent of the two values of the Dirac phase used in the PMNS matrix.

All the Yukawa textures found exhibit the relations given by Eqs. (26)–(28), so an important feature that we want to point out is that the matrices we have found show a very large mixing (nearly $\pi/2$) between the second and third generations of the charged leptons.

4.4. Four-zero textures

We have already explored the textures with three zeros and found that it is possible to have solutions in the allowed ranges for many of them. Now we are interested in checking if this is also possible for textures with four zeros. To start, we list the possible textures with four zeros and their equivalent (column) permutations, discarding those with a row or column completely filled with zeros (thus avoiding singular matrices):

$$\begin{aligned}
 M_{401} &= \begin{pmatrix} 0 & 0 & c \\ 0 & e & 0 \\ g & h & i \end{pmatrix}; & M_{402} &= \begin{pmatrix} 0 & 0 & c \\ 0 & e & f \\ g & h & 0 \end{pmatrix}; & M_{403} &= \begin{pmatrix} 0 & b & c \\ 0 & 0 & f \\ g & h & 0 \end{pmatrix}; & M_{404} &= \begin{pmatrix} 0 & b & c \\ 0 & e & f \\ g & 0 & 0 \end{pmatrix}; \\
 M_{405} &= \begin{pmatrix} 0 & 0 & c \\ d & e & 0 \\ 0 & h & i \end{pmatrix}; & M_{406} &= \begin{pmatrix} 0 & 0 & c \\ d & e & f \\ 0 & h & 0 \end{pmatrix}; & M_{407} &= \begin{pmatrix} 0 & 0 & c \\ d & e & 0 \\ g & h & 0 \end{pmatrix}; & M_{408} &= \begin{pmatrix} 0 & b & c \\ d & 0 & 0 \\ 0 & h & i \end{pmatrix}; \\
 M_{409} &= \begin{pmatrix} 0 & b & c \\ d & 0 & f \\ 0 & h & 0 \end{pmatrix}; & M_{410} &= \begin{pmatrix} a & b & c \\ 0 & 0 & f \\ 0 & h & 0 \end{pmatrix}; & M_{411} &= \begin{pmatrix} 0 & 0 & c \\ 0 & e & f \\ g & 0 & i \end{pmatrix}; & M_{412} &= \begin{pmatrix} 0 & b & 0 \\ d & e & f \\ 0 & h & 0 \end{pmatrix}; \\
 M_{413} &= \begin{pmatrix} a & 0 & c \\ 0 & e & 0 \\ 0 & h & i \end{pmatrix}; & M_{414} &= \begin{pmatrix} a & 0 & c \\ 0 & e & f \\ 0 & h & 0 \end{pmatrix}; & M_{415} &= \begin{pmatrix} 0 & b & c \\ 0 & 0 & f \\ g & 0 & i \end{pmatrix}; & M_{416} &= \begin{pmatrix} a & b & c \\ 0 & 0 & f \\ 0 & 0 & i \end{pmatrix}; \\
 M_{417} &= \begin{pmatrix} a & 0 & c \\ 0 & e & f \\ 0 & 0 & i \end{pmatrix}; & M_{418} &= \begin{pmatrix} 0 & 0 & c \\ 0 & 0 & f \\ g & h & i \end{pmatrix}.
 \end{aligned} \tag{30}$$

We have also calculated the product $M_l M_l^T$ for each texture and we can observe that most of them render one or two zero entries. As in the previous case, this increases the difficulty in finding solutions to the system of equations in Eq. (5). Moreover, since we are assuming only real values in the mass matrix entries, for the four-zero textures we are left with 6 equations and only 5 variables to satisfy them and the system is over-constrained.

The zero entries in the product $M_l M_l^T$ for each texture are the following:

$$\begin{aligned}
 (M_{401} M_{401}^T)_{12} &= 0, & (M_{402} M_{402}^T)_{13} &= 0, & (M_{403} M_{403}^T)_{23} &= 0, & (M_{404} M_{404}^T)_{13,23} &= 0, \\
 (M_{405} M_{405}^T)_{12} &= 0, & (M_{406} M_{406}^T)_{13} &= 0, & (M_{407} M_{407}^T)_{12,13} &= 0, & (M_{408} M_{408}^T)_{12} &= 0, \\
 (M_{409} M_{409}^T)_{23} &= 0, & (M_{410} M_{410}^T)_{23} &= 0, & (M_{413} M_{413}^T)_{12} &= 0, & (M_{414} M_{414}^T)_{13} &= 0.
 \end{aligned}$$

The only textures which give non-zero entries in $M_l M_l^T$ are M_{411} , M_{415} , M_{416} , and M_{417} . Those would be the more interesting cases to study if we allow complex parameters (this would imply also to allow the δ CP-violating phase to take all its possible values). M_{412} , M_{416} and M_{418} also render non-zero entries in $M_l M_l^T$ but they are singular.

We performed a scan over all the allowed experimental range for the mixing angles trying to solve the system of equations for each particular texture, in the case of real parameters, without success. The only possibility is to consider cases where one of the zero entries in the four-zero texture gets slightly turned on. This case could correspond then to one of the three-zero texture above where one of the entries is much smaller than all others. Analyzing the three-zero textures and the relative size of their entries (presented above), we observe that except for M_{304} , all of them contain entries in the range $(10^{-4}-10^{-3})-10^2$ MeV, and that the smallest one is at least two orders of magnitude smaller than the next one. It is then possible, from a model building perspective, to consider a four-zero texture where one of the zeros is *lifted* (perhaps due to radiative corrections, or higher order operator mixings) such that at the end one ends up with one of the successful three-zero textures above. Here we show which four-zero texture could be used in such a scenario

$$\begin{aligned}
 M_{308}(c \sim 0) &\rightarrow M_{402}; & M_{309}(i \sim 0) &\rightarrow M_{403}; & M_{310}(g \sim 0) &\rightarrow M_{402}; \\
 M_{311}(c \sim 0) &\rightarrow M_{406}; & M_{312}(i \sim 0) &\rightarrow M_{409}; & M_{313}(i \sim 0) &\rightarrow M_{406}; \\
 M_{314}(c \sim 0) &\rightarrow M_{414}; & M_{315}(i \sim 0) &\rightarrow M_{410}; & M_{316}(i \sim 0) &\rightarrow M_{414}.
 \end{aligned}$$

As a final remark we comment that even though at this point we considered only real matrices for the charged lepton mass matrices, it is possible to extend some of our results to the case of complex matrices with factorizable phases, i.e. mass matrices that can be written as $M_l = P^* \hat{M}_l P$, where \hat{M}_l are matrices with real entries and P a diagonal phase matrix, $P = \text{diag}(e^{i\phi_1}, e^{i\phi_2}, e^{i\phi_3})$. Then, if \mathcal{O}_l is the orthogonal matrix which diagonalizes $\hat{M}_l \hat{M}_l^T$ we can write, under our assumption $U_\nu = U_{TBM}$, $\mathcal{O}_l = P^* U_{TBM} U_{PMNS}^T$. Nevertheless, from the property of orthogonality and $\det \mathcal{O}_l = \pm 1$ we can infer that the only possible values for the factorizable phases are integer multiples of π . We checked exactly the same three-zero textures as before, but allowing complex entries and a CP-violating phase $\delta = \pi/2$ and found

solutions for the same textures as in the real case. The difference with our previous results is that in these cases solutions are found in all the allowed volume of angles, even for Y_{304} , and the order of magnitude of the entries are generally larger. In the four-zero texture we again find no solutions and due to the fact that the entries in the three-zero textures are larger in this case, it is not possible to easily start from a four-zero texture and lift one zero (here we are thinking of a naturally small correction to the zero entry in question).

5. Conclusions

We analyze several textures for the charged lepton mass matrix under the assumption that the neutrino mass matrix is diagonalized by the TBM matrix, and with the intention of maximizing the number of zeros in them. Requiring the U_{PMNS} mixing matrix to be consistent with the allowed experimental range for mixing angles (fixing the CP-violating phase), and with (the central values of) the charged lepton masses, we explore the maximum number of zeros possible in a texture under the assumption of real charged lepton mass matrix entries. We find that there are ten three-zero textures which provide U_{PMNS} values in agreement with and also determine the size range for their entries. Among the successful textures, the one with zeros in the diagonal shows an interesting behavior in the sense that in order to work, it requires the mixing angle θ_{23} to lie in a very restricted range which, albeit consistent with the experimental range, it excludes the central experimental values.

A general analysis of the successful textures showed that there are relations between their entries and the charged lepton masses. Through a CKM-like parametrization of the U_l mixing matrix we are able to obtain the texture-independent specific relations in terms of the three rotation angles in U_l .

We find no solutions for four-zero textures but observe that it is possible to consider cases where one the zeros is lifted in such a way that the remaining mass matrix corresponds to some of the successful three-zero textures. Finally, we explore a possible extension to consider the cases with complex factorizable textures. We find similar results, i.e. solutions available for the three-zero textures and no solutions for the four-zero texture, with the difference that the typical entry size of the charged lepton mass matrix is generally larger in this case.

While preparing this Letter, a new preprint appeared in the arxiv [18], where an analysis of the charged lepton mixing matrix was performed using the TBM matrix form as well as the Bimaximal Mixing matrix (BM) for the neutrino mixing matrix. They consider the charged lepton mixing matrix to be nearly the identity but deviated from it by one and two parameters for the BM and the TBM case respectively. The parameters are the Cabibbo angles $\lambda = \sin\theta_{12}$ and $\sin\theta_{23}^l$ for the TBM case, assuming that the U_l has its own CKM-like parametrization.

In our case the assumption of U_l as a matrix near the identity is not used. Instead, we determine this matrix by allowing the three rotation angles to vary over the whole experimental range and find that in fact, since $\theta_{23}^l \sim \pi/2$, the matrix is not close to the identity.

Also, in our context, the goal included to find the textures that are diagonalized with Eq. (3). This is not explored in [18] and we feel it is a useful result that can be used by model builders interested in flavor symmetries.

Acknowledgements

M.A.B.-A. thanks Conacyt for a fellowship as a SNI research assistant. A.A. acknowledges support from Conacyt (México).

References

- [1] P.F. Harrison, D.H. Perkins, W.G. Scott, Phys. Lett. B 530 (2002) 167, hep-ph/0202074.
- [2] K. Abe, et al., T2K Collaboration, Phys. Rev. Lett. 107 (2011) 041801, arXiv:1106.2822 [hep-ex].
- [3] Y. Abe, et al., Indication for the disappearance of reactor electron antineutrinos in the Double Chooz experiment, arXiv:1112.6353 [hep-ex].
- [4] F.P. An, et al., Daya Bay Collaboration, Phys. Rev. Lett. 108 (2012) 171803, arXiv:1203.1669 [hep-ex].
- [5] J.K. Ahn, et al., RENO Collaboration, Phys. Rev. Lett. 108 (2012) 191802, arXiv:1204.0626 [hep-ex].
- [6] J. Barry, W. Rodejohann, Nucl. Phys. B 842 (2011) 33, arXiv:1007.5217 [hep-ph].
- [7] L. Dorame, D. Meloni, S. Morisi, E. Peinado, J.W.F. Valle, Nucl. Phys. B 861 (2012) 259, arXiv:1111.5614 [hep-ph].
- [8] S. Morisi, J.W.F. Valle, Neutrino masses and mixing: a flavour symmetry roadmap, arXiv:1206.6678 [hep-ph].
- [9] P.H. Frampton, S.L. Glashow, D. Marfatia, Phys. Lett. B 536 (2002) 79, hep-ph/0201008.
- [10] H. Fritzsch, Z.-z. Xing, S. Zhou, JHEP 1109 (2011) 083, arXiv:1108.4534 [hep-ph].
- [11] C. Hagedorn, W. Rodejohann, JHEP 0507 (2005) 034, hep-ph/0503143.
- [12] H. Fritzsch, Phys. Lett. B 70 (1977) 436;
H. Fritzsch, Phys. Lett. B 73 (1978) 317.
- [13] G. Ahuja, M. Gupta, M. Randhawa, R. Verma, Phys. Rev. D 79 (2009) 093006, arXiv:0904.4534 [hep-ph].
- [14] N. Mahajan, M. Randhawa, M. Gupta, P.S. Gill, Investigating texture six zero lepton mass matrices, arXiv:1010.5640 [hep-ph].
- [15] M. Gupta, G. Ahuja, Int. J. Mod. Phys. A 26 (2011) 2973, arXiv:1206.3844 [hep-ph].
- [16] K. Nakamura, et al., Particle Data Group Collaboration, J. Phys. G 37 (2010) 075021, and 2011 partial update for the 2012 edition, URL: <http://pdg.lbl.gov>.
- [17] T. Schwetz, M. Tortola, J.W.F. Valle, New J. Phys. 13 (2011) 109401, arXiv:1108.1376 [hep-ph].
- [18] C. Duarah, A. Das, N. Nimai Singh, Charged lepton contributions to bimaximal and tri-bimaximal mixings for generating $\sin\theta_{13} \neq 0$ and $\tan^2\theta_{23} < 1$, arXiv:1207.5225v1 [hep-ph].